Crystallographic Analysis of Nucleation at Hardness Indentations in High-Purity Aluminum

Xu, Chaoling; Zhang, Yubin; Lin, Fengxiang; Wu, Guilin ; Liu, Qing; Juul Jensen, Dorte

Published in:
Metallurgical and Materials Transactions A - Physical Metallurgy and Materials Science

Link to article, DOI:
10.1007/s11661-016-3704-3

Publication date:
2016

Document Version
Peer reviewed version

Crystallographic Analysis of Nucleation at Hardness Indentations in High Purity Aluminum

C.L. Xu[1,2*], Y.B. Zhang[2], F.X. Lin[2], G. L. Wu[1], Q. Liu[1], D. Juul Jensen[2]

[1] College of Material Science and Engineering, Chongqing University, Chongqing 400044, China

[2] Section for Materials Science and Advanced Characterization, Department of Wind Energy, Technical University of Denmark, Risø Campus, DK-4000 Roskilde, Denmark

*corresponding author: chaoxu@dtu.dk

Abstract: Nucleation at Vickers hardness indentations has been studied in high purity aluminum cold rolled 12%. Electron channeling contrast was used to measure the size of the indentations and to detect nuclei, while electron backscattering diffraction was used to determine crystallographic orientations. It is found that indentations are preferential nucleation sites. The crystallographic orientations of the deformed grains affect the hardness and the nucleation potentials at the indentations. Higher hardness gives increased nucleation probabilities. Orientation relationships between nuclei developed at different indentations within one original grain are analyzed and it is found that the orientation distribution of the nuclei is far from random. It is suggested that it relates to the orientations present near the indentation tips which in turn depend on the orientation of the selected grain in which they form. Finally possible nucleation mechanisms are briefly discussed.

Keywords: nucleation of recrystallization, aluminum, orientation relationships, indentations

1 Introduction

Nucleation of recrystallization in the bulk of metals is very difficult to control and uncertainties exist on active nucleation mechanisms [e.g. 1, 2]. However it is well known that surface imperfections such as scratches and hardness indentations stimulate nucleation. The present work deals with the latter. Extensive studies have been done to understand the deformation mechanism occurring during indenting [e.g. 3-5]. Early work focused on the visualization of the deformation microstructures of the volume underneath indentations using split samples and optical microscopy [6, 7]. Newer studies use scanning electron microscopy and conventional electron backscattering diffraction (EBSD) [8] as well as 3D-EBSD [9] to investigate the size of the affected zone underneath indents. It is generally found that hardness indentations cause a high local dislocation density.

Also several studies have investigated nucleation at hardness indentations [e.g. 10-13]. Upon annealing, the increased dislocation density in indentation zones provides a higher driving force for nucleation and subsequent growth during recrystallization. It has been found that recrystallization depends strongly on the distribution of stored energy below the indentations and that the recrystallized volumes closely match the indentation zones [11]. It has also been found that the shape of the indenter also has an effect on the nucleation potentials: a sharp indenter leads to more nucleation than a ball shaped one [13]. Although it is well documented that hardness indentations stimulate nucleation, much less is known about crystallographic effects. Open questions include

(1) Do grains of different crystallographic orientations have the same potential for stimulating nucleation at hardness indentations?

(2) Do all nuclei that form at different hardness indentations within a given grain have the same crystallographic orientation?
(3) What orientation relationships exist between nuclei and matrices?

Questions No.1 addresses nucleation potentials and thus nucleation densities which determine the average recrystallized grain size. Question No.2 and 3 address crystallographic orientation relationships and thus the formation of texture. Furthermore question No.3 may shed light on potential nucleation mechanisms. The latter is critically needed in recrystallization modeling in which proper nucleation mechanisms are rarely included and it is generally assumed that nuclei have random orientations or orientations as deformed microstructures [14].

In the present work, the above 3 questions are studied for nucleation of a lightly cold rolled, coarse grained pure aluminum sample further deformed locally by a large number of Vickers hardness indentations in each grain.

2 Experimental

A polycrystalline aluminum sheet of 99.996% purity with a size of 94 × 46 × 3 mm^3 was used. The initial average grain diameter was ≈300 μm. This grain size was too fine for the planned experiment in which several hardness indentations with sizes of 160 μm -190 μm along the diagonal lines have to be done within each grain to study possible grain orientation effects on nucleation potentials. Therefore the sheet was ground to 4000# SiC paper and electro-polished, followed by annealing at 863 K (600 °C) for 7 days. The grain sizes after this annealing were in the range from 500 μm to 7 mm, which is ideal for the present experiment. Then the sheet was cold rolled 12% in two passes, each with the geometric parameter l/h around 2, where l is the contact length between the rolls and the sample and h is the average sample thickness before and after each pass; thus the deformation is expected to be relatively homogeneous through the sample thickness [15]. This light rolling ensures that nuclei forming at indentations can grow to a decent size outside the indented zone, easing the detection and analysis. Next, 6 samples sized 6.0 × 4.0 × 1.3 mm^3 were prepared from the sheet. In total, 13 large grains with different orientations (marked A to M) were selected in these samples. Each sample was ground and electro-polished with extreme care to remove surface imperfections, especially scratches, to avoid nucleation from such sites. All samples were kept in a freezer when not in use.

Hardness indentations were done on all samples on the RD-TD plane using a Vickers diamond indenter of pyramidal shape, with a square base and an angle of 136° between opposite faces, using a force of 500 g. All the indentations were positioned far away from grain boundaries and the distance between two indentations was larger than $3d$, where d is the length of the diagonal lines of the indentations, thereby avoiding overlap of deformation zones.

Electron channeling contrast (ECC) was used to measure the length of the diagonal lines of the indentations, and the hardness HV (Kgf/mm^2) was calculated as:

$$HV = 2F\ sin\frac{136^\circ}{2} / \left(\frac{d_1+d_2}{2}\right)^2. \quad (1)$$

F is the force of hardness test, and d_1 and d_2 are the length of the two diagonal lines.

Before annealing, the deformation microstructure of each grain far away from the indentations was characterized by EBSD using a Zeiss Supra 35 thermal field emission gun scanning electron microscope (FEG-SEM). Five samples containing the selected 13 grains (grains B-M plus approximately ½ of grain A) were annealed at 583 K (310 °C) for 1 hour. The samples were wrapped in baking paper before annealing to avoid scratches during sample handling. After annealing, the area around each indentation was characterized by EBSD to measure the orientations of nuclei and the recovered matrix around them. This was done at the sample surfaces. Whereas the EBSD measurements clearly reveal nuclei at the sample surfaces, nuclei which have formed below the surfaces (for example near tips) but not yet grown very large, cannot be detected by this method. Therefore ECC was used to observe if there were small nuclei 'inside the indentations'.

Orientation relationships between nuclei and surrounding recovered matrix as well as between nuclei from the same grain were analyzed based on EBSD maps. It should be noted that twins within a nucleus are not counted as separate nuclei here. If two neighboring nuclei are twin related to each other and one of them has special relationships to the deformed matrix, such as misorientation angles below 15°, 40°<111> or 60°<111>, this one is considered as a nucleus while the other one is not. If both of them have no special relationships to deformed matrix, the one with the larger size is counted as a nucleus.

The sixth sample containing half of grain A was cut into 2 parts (along the rolling plane into a top and a bottom part). Indentations were done on both the top and bottom part as described above. The top part was used for serial sectioning to characterize the deformation microstructure underneath the indentations and the bottom part for annealing at 583 K (310 °C) for 2 minutes only. The serial sectioning was done by repeated grinding, mechanical polishing and EBSD measurements. The sample annealed for 2 minutes was ground and electro-polished to a section near the indentation tips, followed by EBSD characterization.

3 Results

3.1 Nucleation potentials at indentations in grains of different orientations

The average orientation and the orientation spread within the deformation microstructures far away from the indentations of each grain were calculated from the EBSD data and the values are reported in table 1. Most grains contained extended planar dislocation boundaries, while some grains only revealed cell structures. Examples of grains with dislocation boundaries and with a cell structure are shown in figure 1. These observations agree well with previous observations in polycrystalline aluminum cold rolled to a low strain [16-18].

In total 108 hardness indentations were made in the 13 grains and 37 of them in 8 grains were observed to stimulate nucleation. Most of the 'nucleating indentations' stimulated one nucleus, while 9 indentations stimulated 2 nuclei. No nuclei were detected away from the indentations, which is in good agreement with previous investigations [e.g. 10, 17]. Table 1 gives an overview of the nucleation observed within all the 13 grains.

3.2 Orientation relationships between nuclei formed at different hardness indentations within each grain

The nuclei formed within each grain were analyzed to investigate possible orientation relationships between the nuclei. This was only relevant for grain A, C, H, I and F that stimulated at least 6 nuclei (see table 1). The nuclei within grain A, C and I were scattered but still far from random. As an example, the orientations of all nuclei observed in grain A are shown in figure 2a. The orientations of the nuclei in grain F and H appeared to be less scattered (see figure 2b), but this may be an effect of statistics. When comparing the pole figures in figure 2, it is clear that the orientation distributions are different; i.e. grains with different orientations appear to give nuclei with different orientations.

3.3 Orientation relationships between nuclei and matrix

The microstructures around the nuclei were characterized using EBSD and the orientation relationships between the nuclei and the surrounding matrix were analyzed. In total, 24 (53%) nuclei were surrounded partly by low angle boundaries (LABs) below 15°. The other 21 nuclei (47%) were surrounded only by high angle boundaries (HABs) and17 of these had a common rotation axis near a <100> axis, 3 near a <111> axis, while one was rotated around a <120> axis.

These results were obtained at the surface of samples for nuclei which all have grown to fairly large sizes. According to our previous preliminary results, nuclei might form near indentation tips [17]. It is, thus, likely that the nuclei analyzed above formed below the surface and grew to be visible at the surface. To investigate this, the bottom half of sample 6 (containing grain A) was annealed at 583 K (310 °C) for 2 minutes to explore where the nuclei formed and what orientations they had.

By using ECC, 4 small nuclei (to be called 2-minutes nuclei) numbered n1, n2a, n2b and n3 (the numbers represent the indentation number, and the lower case n is used to signal that these nuclei developed after the short annealing time as opposed to the capital N for the long annealing time), were observed at 3 indentations as shown in figure 3. All the nuclei were about 30 μm in diameter, which was much smaller than the size of the indentations and they were all located near the indentation tips as shown in figure 3a, c and e. Therefore, the sample was ground and electro-polished to reveal areas near the indentation tips, and then the orientations of the nuclei and the surrounding recovered matrix were examined using EBSD as shown in figure 3b, d and f.

It is found that all the four nuclei formed *both* LABs and HABs to the recovered matrix. This is in contrast to the surface observations of the 1-hour nuclei (53% of them are surrounded by HABs only). To compare the two cases, the orientations of all the 1-hour and 2-minutes nuclei were plotted together in a pole figure shown in figure 2a. It reveals that nucleus n3 had an orientation similar to nuclei N9 and N18. Although the orientations of nuclei n1, n2a and n2b were not the same as any 1-hour nuclei, their misorientation angles with nucleus N18 were still relatively small. It is therefore likely that the 1-hour nuclei also formed with orientations similar to the matrix at sites near the indentation tips. This hypothesis was tested by looking at orientation relationships between the 2-minutes nuclei and the matrix far away from them — corresponding to the misorientation relationships that would be observed if they had been annealed to grow to sizes as large as the 1-hour nuclei. In the EBSD maps of figure 3, the color of each pixel is defined by its angular orientation deviation from the nucleus. It can be observed that the misorientation angles between nucleus n1 and the recovered matrix 80 μm away from it were lower than 15° (green in figure 3b).Therefore, it can be expected that when nucleus n1 grows into a size of about 160 μm, the nucleus will be surrounded by LABs. This is similar to nucleus N17. On the other hand, the nuclei n2a, n2b and n3 in figure 3d and f will form only HABs to the surrounding matrix when they have grown to a size similar to the 1-hour

nuclei. These results thus support the hypothesis that the 1-hour nuclei form near the indentation tips with orientations already present there.

4 Discussion

4.1 Nucleation at hardness indents

In undeformed materials it is well known that the hardness depends on the crystallographic orientations of the grains [19], and that areas near grain boundaries may differ from grain interiors [e.g. 20]. In the present work, a weakly rolled sample is investigated. The hardness will therefore not only depend on the initial grain orientations, but also on the rolled microstructures. Such microstructures are known to be subdivided by deformation induced extended dislocation boundaries as well as cells. Misorientations across the geometrically necessary dislocation boundaries are generally higher than those across incidental cell boundaries [21]. On the micrometer scale the microstructure is therefore inhomogeneous and varies from place to place. The rolled microstructure is also determined by the initial grain orientations, so although the general principles of subdivision are the same, the deformation microstructures vary from grain to grain too [18, 22, 23].

In other words, the initial grain orientations determine the rolled microstructures and are expected to affect the hardness. For the present 13 grains this is validated by relating the measured hardness to the energy stored in the rolled deformation microstructures far away from indentations calculated based on the measured misorientations ≥ 2° across dislocation boundaries using the method described in [24]. As illustrated in figure 4, the grains with higher stored energies, as expected have higher hardness values. The scatter in hardness (expressed as error bars in figure 4) within each grain is likely to be a consequence of the rolling and thus the local variations within the grains. The figure reveals that grains with similar stored energies, e.g. grain B and D, can have very significantly different hardness, which is likely to be a grain orientation effect.

The stored energy in the deformed matrix is known to provide the driving force for nucleation and growth during recrystallization. As shown above it is relatively straightforward to determine the stored energy at locations far away from the indentations. At the indentations the energies cannot be estimated using 2D measurements because of the complicated 3D deformation volumes underneath indentations. Generally one may assume, however, that a large indentation (small hardness value) means that the local volume under the indentation is in a state favorable for the indenting deformation, which in turn may lead to relative lower dislocation densities and thus lower stored energies at that site. Based on this assumption, the average hardness value of each grain is related to the corresponding nucleation probability (see figure 5a). The curve has a large scatter, but the general trend is that the nucleation potential increases with increasing hardness values. To further investigate the possible relationship between hardness and nucleation potentials, figure 5b shows the nucleation percentages at all the hardness indentations The figure reveals a clear tendency that indentations with higher hardness stimulate more nuclei and vice versa.

The detailed analysis of grain A, suggests that the nuclei develop preferentially at sites near the indentation tips (see figure 3). This may be explained by the distribution of stored energies around the indentation. The unannealed top half of sample 6 with grain A was sectioned to reveal the deformation microstructures at different depths of a volume near a hardness indent (see figure 6). It is evident that the spacing of the dislocation boundaries within the indentation zone is smallest at the section close

the indentation tip (figure 6d), and that more HABs form there – i.e. the stored energy is higher in the section close to the tip than at other sections. Furthermore in the tip section, the stored energy is highest at the tip center and decreases with increasing distance (see figure 7).This observed distribution of stored energy agrees with a model developed by Nix and Gao [25] and Swadener's results [26]. Nucleation would be facilitated by locally high stored energy as well as by a gradient in stored energy. The latter would mean that the preferential nucleation site is at the maximum stored energy and the growth of a nucleus formed here will not be hindered by impingements with other nuclei because fewer or no nuclei will form in the neighbouring regions of lower stored energy. This agrees well with the present observations and analysis, that the nucleation potential is higher for higher hardness (see figure 5), and the indentation tip is the preferred nucleation site. The present samples were cold rolled before indenting and it therefore cannot be excluded that the local microstructures developed during rolling have an influence on the nucleation potentials at the indentations. Table 1 indicates that deformed microstructures with extended planar dislocation boundaries (EPB) may have a better chance to stimulate nucleation than those with a cell structure (CS).

4.2 Orientation relationships

For all the investigated grains the nuclei are observed near the hardness indentations, and even though the nuclei form at different hardness indentations within a given grain, their orientations are related - in the sense that they are within limited orientation distributions and not randomly scattered. It is thus very likely that the orientations of the nuclei are related to the matrix in which they form. As discussed above the indentation tips appear to be the most potential sites with the highest stored energy (see figure 7). This is in agreement with the detailed TEM investigations near Vickers indentation tips which revealed severe deformation at the tips and along the diagonal lines [12]. Upon annealing big subgrains preferentially developed within these severely deformed regions [12]. In the present work the short time annealing revealed nuclei only near the indentation tip. It is thus of interest to evaluate possible correlations between the orientations of the nuclei and the orientations present at the tips and along the diagonal lines. This can for the present data be done for grain A.

For this analysis, the area near the indentation tip is divided into 4 parts: I, II, III and IV (see figure 8a). The orientations here and the orientations of all 1-hour and 2-minutes nuclei found in grain A are plotted in <100> pole figures (see figure 8b-e). The figures reveal that the 4 parts I-IV have somewhat different orientations. It may seem odd that the 4 parts in a symmetrical Vickers diamond indentation lead to somewhat different crystallographic orientations and, as shall be discussed below, to different stored energies in the 4 parts of the deformation microstructure near the tip of the indented zone. Two factors are important here: ① the orientation of grain A is {3-1-1}<215>, which means that the 4 sides of the indenter push against different orientations and the 4 sides are therefore deformed with forces of different directions. The indenter strain direction will thus be different in the 4 parts and shift the crystallographic orientations in different directions. ② the sample was cold rolled 12% before the indentation so local variations due to this rolling deformation will be present in the microstructure [24].

Figure 8b-e clearly reveals that the orientations of most of the nuclei are found within the orientation spread of region I and IV, and a few at the outskirts of the orientation spread of region III. Following the idea above concerning relationship between nucleation potentials and local stored energies, the stored energy within the I-IV regions are calculated. The results are 0.14 MJ/m^3, 0.04 MJ/m^3, 0.16

MJ/m^3, and 0.23 MJ/m^3 within the four regions, respectively. The stored energy of region II is very low and no nuclei form there. Region I, III and IV have higher stored energy. Many nuclei have orientations as inregion I and IV and are thus likely to have formed there, while fewer in region III. By comparing the microstructures within regions I, III, IV (see figure 8a), it is clear that I and IV have banded structures with alternating orientations while region III appears more homogeneous. It is thus suggested that not only the stored energy but also the morphology of the deformation microstructure affect the nucleation potentials.

The mechanism(s) leading to nucleation cannot directly be quantified from the present work. However as the nuclei appear to have orientations very similar to those present at the active nucleation sites, conventional mechanisms such as coalescence [27], strain induced boundary migration (SIBM) [28, 29] and subgrain growth [30-32] could explain the results. It should be noted that as no original grain boundaries are present near the nuclei, the SIBM mechanism should here refer to strain induced *dislocation* boundary migration.

Most of the nuclei characterized in the present work have grown to quite large sizes. It can therefore not be ruled out that possible preferential growth might have affected our results. For the present nuclei, it is however observed that the majority have a nearer 30° <100> than e.g. a 40° <111> misorientation relationship to the matrix. As the 30° <100> misorientation is not expected to lead to fast boundary migration, preferential growth is not expected to be of major concern for the present results.

5. Conclusions

The nucleation in weakly rolled aluminum further deformed locally by well distributed hardness indentations has been investigated. Thirteen big grains each with several hardness indentations were characterized after annealing leading to nucleation of recrystallization. It can be concluded that:

1. All nuclei were observed at the hardness indentations, which is expected as the stored energy here is significantly higher than in the surrounding rolled matrix microstructures.
2. Hardness indentations in only 8 of the 13 investigated grains were observed to stimulate nucleation. The general trend is that grains with higher hardness values are more prone to stimulate nucleation than those with lower hardness values. As the orientations of the grains are known to determine the evolution of the deformation microstructure after e.g. rolling, orientations are also very likely to affect the more complex deformation microstructures underneath hardness indentations, and higher hardness values may lead to higher dislocation densities and thus higher stored energies stimulating the nucleation. For the present samples, which are rolled before indentation, it is suggested that besides the local stored energies also the morphology of the deformation microstructures may affect the potential for nucleation.
3. The orientations of the nuclei from different indentations in a given grain are observed not to be randomly distributed, but clustered in limited orientational spaces. The nuclei orientations are related to the orientations present in the complex deformed matrices near the tips of the indentations. Nucleation by mechanisms such as subgrain coalescence, strain induced dislocation boundary migration or subgrain growth could thus lead to nuclei with orientations as those observed in the present work.
4. When only inspected on the surface, most of the nuclei are observed to have large misorientations to the matrix, although they have orientations similar to the matrix below the

surface. This underlines the importance of careful 3D or even better 4D (x,y,z,t) experimental investigations of nucleation in samples as the present ones.

Acknowledgements

All authors gratefully acknowledge the support from the Danish National Research Foundation (Grant No.DNRF86-5) and the NSFC of China (Grant No. 51261130091) to the Danish-Chinese Center for Nanometals. Valuable assistance in data analysis from Andy Godfrey, Xuehao Zhen and Jun Sun is highly appreciated.

References

[1] R.D. Doherty, D.A. Hughes, F.J. Humphreys, J.J. Jonas, D. Juul Jensen, M.E. Kassner, W.E. King, T.R. McNelley, H.J. McQueen, A.D and Rollett: Mater. Sci. Eng. A, 1997, Vol.7, pp. 1564-83.
[2] H Paul, M.M. Miszczyk and J H Driver: 36th Risø International Symposium on Materials Science, IOP Conference Series: Mater. Sci. Eng., 2015, Vol. 89, pp. 012010.
[3] T.O. Mulhearn: J. Mech. Phys. Solids, 1959 Vol. 7, pp. 85-96.
[4] M. Rester, C. Motz and R. Pippan: Scripta Mater., 2008, Vol. 59, pp. 742-5.
[5] A.S. Keh: J. Appl. Phys., 1960, Vol. 31, pp. 1538-45.
[6] R. Hill, E.H. Lee and S.J. Tupper: Proc. Roy. Soc., 1947, Vol. 191, pp. 278-303.
[7] L.E. Samuels and T.O. Mulhearn: J. Mech. Phys. Solids, 1957,Vol. 5, pp. 125-34.
[8] M. Rester, C. Motz and R. Pippan: Acta Mater., 2007, Vol. 55, pp. 6427-35.
[9] E. Demir, D. Raabe, N. Zaafarani and S. Zaefferer: Acta Mater., 2009, Vol. 57, pp. 559-69.
[10] C. Zambaldi, F. Roters, D. Raabe and U. Glatzel: Mater. Sci. Eng. A, 2007, Vol. 454-455, pp. 433-40.
[11] G. Xie, L. Wang, J. Zhang and L.H. Lou: Scripta Mater., 2011, Vol. 66, pp. 378-81.
[12] F. Granzer and G. Haase: Zeitschrift fiir Physik, 1961, Vol. 162, pp. 468-82.
[13] D. Eylon, A. Rosen and S. Niedzwiedz: Acta Metall., 1969, Vol. 17, pp. 1013-19.
[14] J. Gruber, H.M. Miller, T.D. Hoffmann, G.S. Rohrer and A.D. Rollett: Acta Mater., 2009, Vol. 57, pp. 6102-12.
[15] O. Mishin, B. Bay , G. Winther and D. Juul Jensen: Acta Mater., 2004, Vol. 52, pp. 5761-70.
[16] Q. Liu, D. Juul Jensen and N. Hansen: Acta mater., 1998, Vol. 46, pp. 5819-38.
[17] C.L. Xu, Y.B. Zhang, G.L. Wu, Q. Liu and D. Juul Jensen: 36th Risoe International Symposium on Materials Science, IOP Conference Series: Mater. Sci. Eng., 2015, Vol. 89, pp. 012054.
[18] N. Hansen and X. Huang : Acta Mater., 1988, Vol. 46, pp. 1827-36.
[19] J.J. Roa, G. Fargas, A. Mateo and E. Jimenez-Pique: Mater. Sci. Eng. A, 2015, Vol. 645, pp. 188-95.
[20] V. Randle, N. Hansen and D. Juul Jensen: Phil. Mag. A, 1996, Vol. 73, pp. 265-82.
[21] N. Hansen and D. Juul Jensen: Mater. Sci. Tech., 2011, Vol. 27, pp. 1229-40.
[22] X. Huang and G. Winther: Phil. Mag., 2007, Vol. 87, pp. 5189-214.
[23] F.X. Lin, A. Godfrey and G. Winther: Scripta Mater., 2009, Vol. 61, pp. 237-40.
[24] A. Godfrey, O. Mishin and T.B. Yu: 36th Risoe International Symposium on Materials Science, IOP Conference Series: Mater. Sci. Eng., 2015, Vol. 89, pp. 012003.
[25] W.D. Nix and H.J. Gao: J. Mech. Phys. Solids, 1998, Vol. 46, pp. 411-25.
[26] J.G. Swadener, E.P. George and G.M. Pharr: J. Mech. Phys. Solids, 2001, Vol. 50, pp. 681-94.
[27] J.C.M. Li: J. Appl. Phys.,1962, Vol. 33, pp.2958-65.
[28] P.A. Beck and P.R. Sperry: J. Appl. Phys., 1950, Vol. 21, pp.150-2.
[29] J.E. Bailey and P.B. Hirsch: Proc. Roy. Soc. A, 1962, Vol. 267, pp. 11-30.
[30] R.W. Cahn: Proc. Phys. Soc. A,1950, Vol. 63, pp. 323-6.
[31] P.A. Beck: J. Appl. Phys., 1949, Vol.20, pp.633-4.
[32] A.H. Cottrell:Progr. Met. Phys., 1953, Vol.4, pp.205-64.

Figure and table captions:

Figure 1 The deformation microstructures far away from indentations of (a) grain A and (b) grain E. The color of each pixel in the maps is given by the orientation deviation (misorientation axis) from the average orientation of this map (see the insert for color explanation).

Figure 2 (a) The orientation distribution of all nuclei developed near indentations in grain A in the samples annealed for 1 h and for 2 minutes. The 2-minutes nuclei will be described in section 3.3. The number refers to the indentation number. The black and red markers represent the 1-hour and the 2-minutes nuclei, respectively. (b) Orientation distributions of the nuclei formed in grain F.

Figure 3 ECC images (a), (c) and (e) and EBSD orientation maps (b), (d), and (f) of four nuclei formed at the tips of indentations in grain A after annealing at 583 K for 2 minutes. The nuclei are marked by red circles and arrows in the ECC images and orientation maps, respectively. In the orientation maps, the white lines represent LABs (≥ 2° and < 15°), while the black lines represent HABs (≥ 15°). The color of each pixel in (b), (c) and (d) is defined by its orientation deviation (angular deviation) from the orientations of the nuclei n1, n2a and n3, respectively (seen as blue grains); see the insert in (f) for color explanation.

Figure 4 The hardness values of all 13 grains as a function of the stored energy in the rolled microstructures far away from indentations measured at the sample surface.

Figure 5 (a) The nucleation potential expressed in percentages for the 13 grains as a function of the average hardness values. (b) The nucleation frequency of indentations as a function of hardness values. It includes all hardness indentations in the 13 grains.

Figure 6 The deformation microstructures at an indentation in grain A at different depth underneath the sample surface: (a) 0 μm (sample surface), (b) 9 μm, (c) 24 μm and (d) 28 μm (at the tip of the indentation). The color of each pixel in the orientation maps is defined by the crystallographic orientations along the sample normal direction, LABs (2–15°) and HABs are shown by thin white and thick black lines, respectively. In (d) the deformation microstructure is divided into regions, marked as R*i*, (*i*=1-5), within which the stored energy is calculated and shown in figure 7.

Figure 7 Stored energies of the areas shown in figure 6d as a function of the distance away from the indentation tip.

Figure 8 (a) EBSD maps of the deformation microstructure near the tip of an indentation in grain A showing four regions. (b)-(e) show {100} pole figures of all the 1-hour and 2-minutes nuclei together with the orientation within the 4 regions in (a).

Table 1 Overview of the nucleation behavior of the 13 grains investigated. The hardness is averaged over all indentations in that grain and the nucleation potentials are given as indentations leading to nucleation (in number and pct.). The data refer to surface observations. EPB and CS are used to describe the deformation microstructures far from the indentations and are short for extended planar boundary microstructures and cell microstructures.

Fig. 1

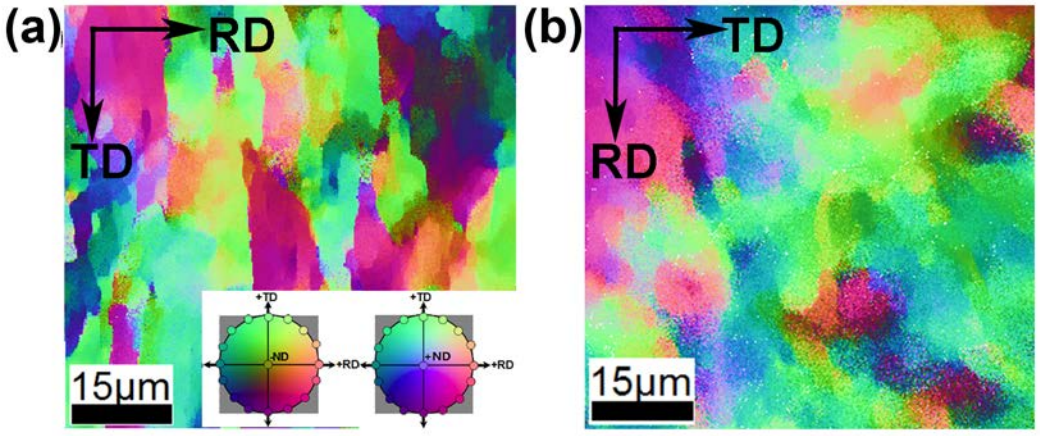
(a)
RD
TD
15μm
+TD
+ND
+RD
(b)
TD
RD
15μm

Fig. 2

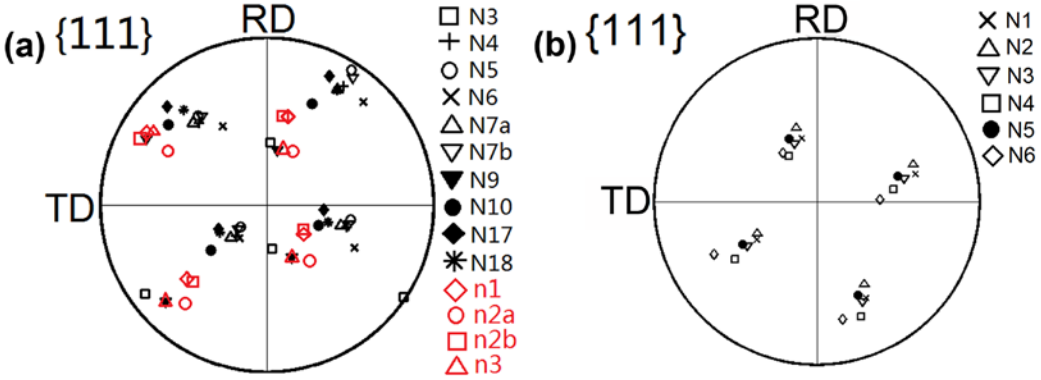
(a) {111}
RD
TD
N3
N4
N5
N6
N7a
N7b
N9
N10
N17
N18
n1
n2a
n2b
n3
(b) {111}
RD
TD
N1
N2
N3
N4
N5
N6

Fig. 3

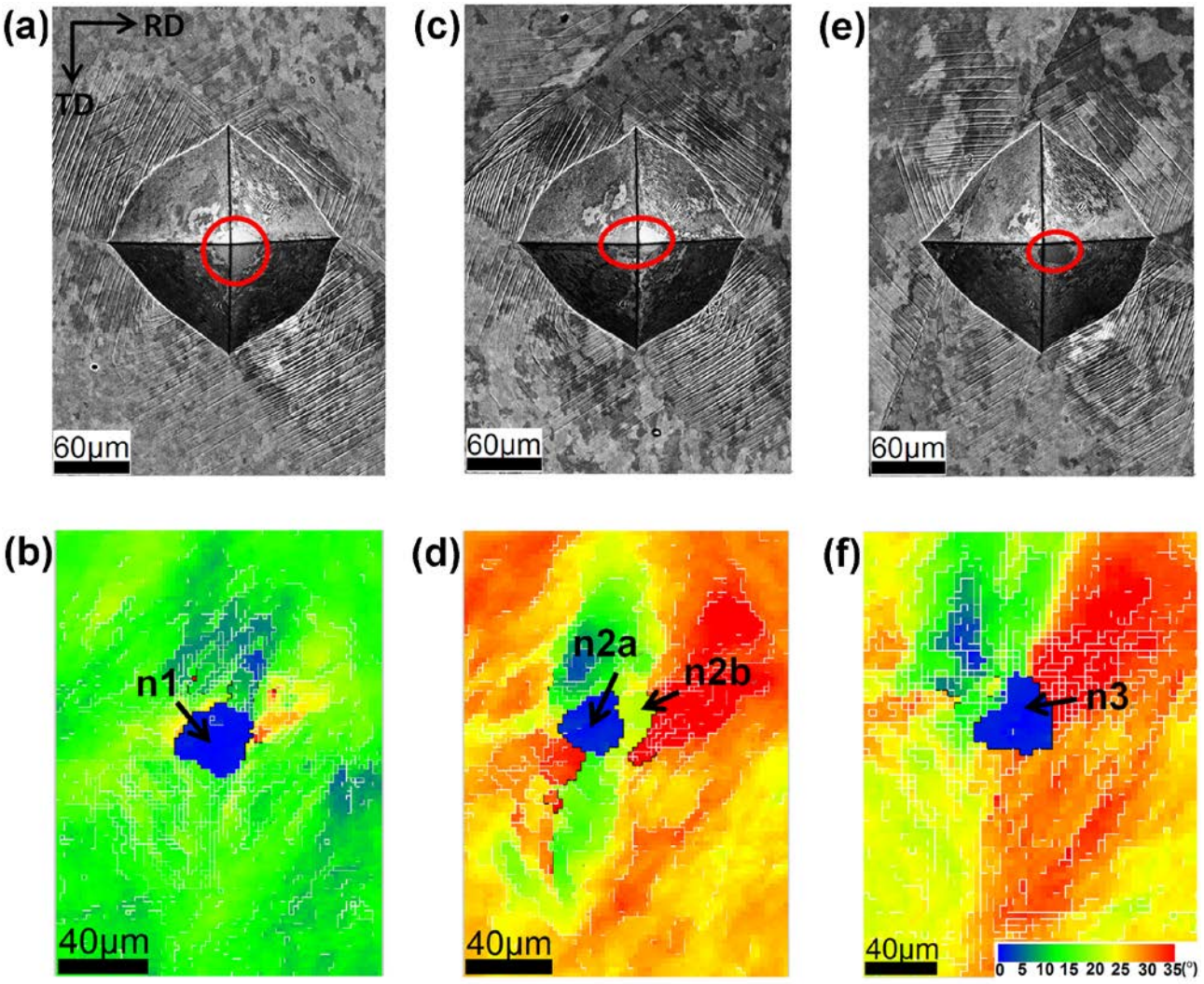
(a)
RD
TD
60μm
(c)
60μm
(e)
60μm
(b)
n1
40μm
(d)
n2a
n2b
40μm
(f)
n3
40μm
0 5 10 15 20 25 30 35(°)

Fig. 4

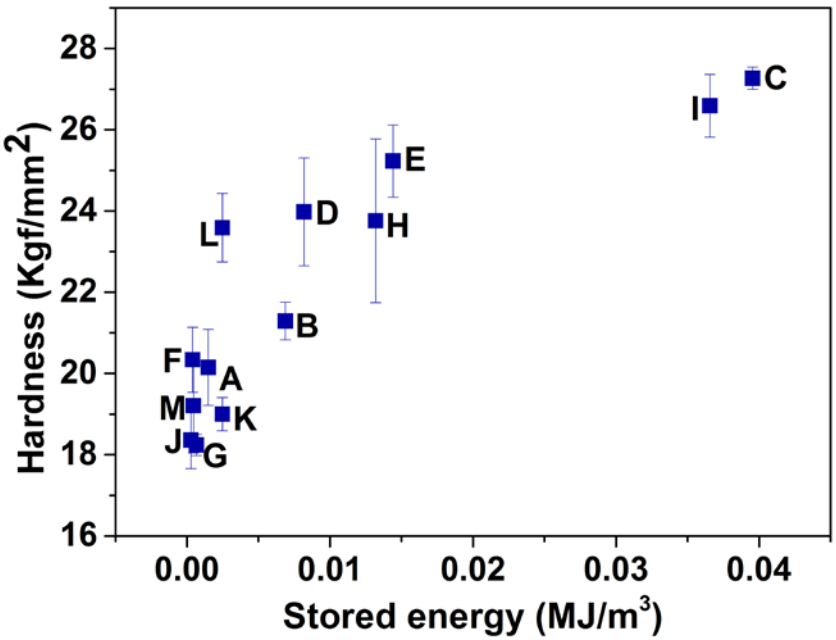
Hardness (Kgf/mm^2)
Stored energy (MJ/m^3)
28
26
24
22
20
18
16
0.00
0.01
0.02
0.03
0.04
C
I
E
D
H
L
B
F
A
M
K
J
G

Fig. 5

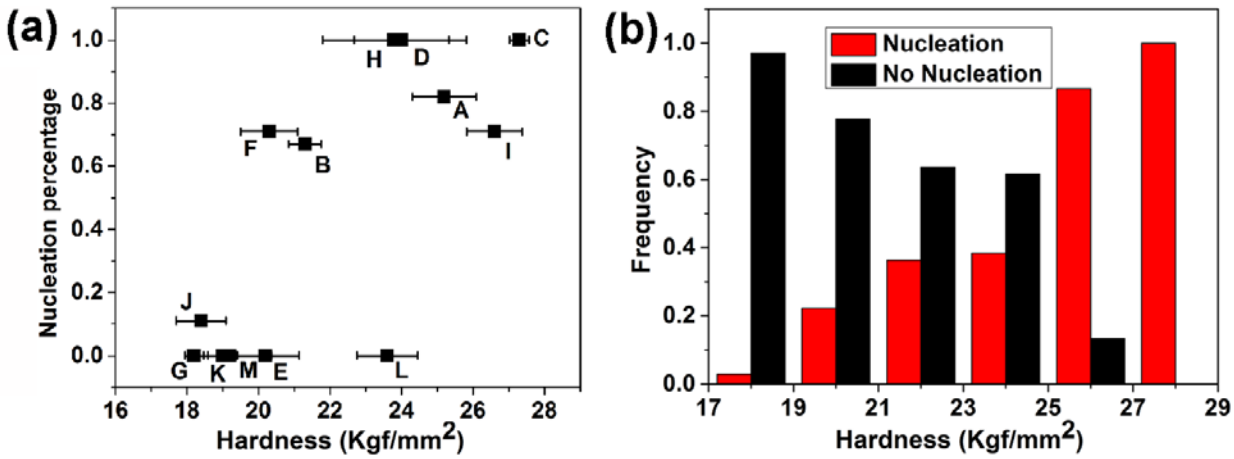
(a)
Nucleation percentage
Hardness (Kgf/mm^2)
1.0
0.8
0.6
0.4
0.2
0.0
16
18
20
22
24
26
28
H
D
C
A
F
B
I
J
G
K
M
E
L
(b)
Nucleation
No Nucleation
Frequency
Hardness (Kgf/mm^2)
1.0
0.8
0.6
0.4
0.2
0.0
17
19
21
23
25
27
29

Fig. 6

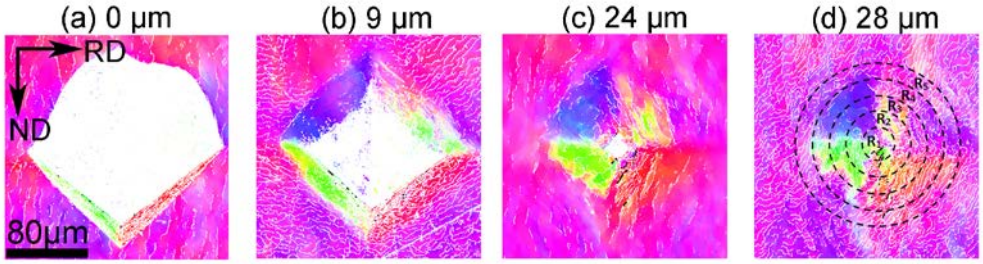

Fig. 7

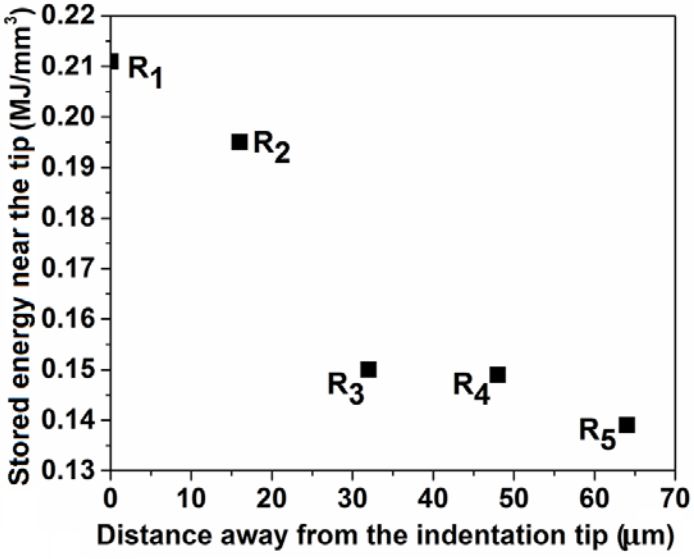

Fig. 8